

# Formation of the Pore Structure of Zirconium Dioxide at the Stage of Gel Aging

V. Yu. Gavrilov and G. A. Zenkovets

*Boreskov Institute of Catalysis, Siberian Division, Russian Academy of Sciences, Novosibirsk, 630090 Russia*

Received November 13, 1998

**Abstract**—The formation of the pore structure of zirconium dioxide at the gel aging stage in an intermicellar medium is studied. The processes, which occur in the course of aging, and the features of the structure formed depend on the pH of gel precipitation. The calcination of  $\text{ZrO}_2$  at 500°C is accompanied by the diffusion process of bulk sintering, which results in a substantial reconstruction of the pore space of the xerogel.

## INTRODUCTION

Zirconium dioxide is widely used as a support for catalysts that usually operate at high temperatures [1–4]. For example, zirconium-based binary oxide systems are used as solid electrolytes [5], including electrolytic membranes for catalytic processes [6], and catalyst supports [7, 8]. For the last few years, zirconium dioxide has been gaining interest as a selective ion-exchanger with controlled sorption properties [9].

An important and topical direction of  $\text{ZrO}_2$  use is associated with a novel catalytic process that has been intensively developed of late. This is the isomerization of normal paraffins  $\text{C}_7\text{--C}_9$  to branched hydrocarbons [10], which enhances the octane number of gasoline without use of aromatic compounds. New active super-acids of the  $\text{SO}_4^{2-}/\text{ZrO}_2$  type have been proposed as catalysts for this process.

It is obvious that the pore structure of zirconium dioxide plays an important role in all of its applications. It is well known that the regularities of the pore structure formation are largely determined by the preparation procedure.

Conventional precipitation is the most common method to obtain  $\text{ZrO}_2$  [11]. Earlier, we have studied the effect of the conditions of the  $\text{ZrO}_2$  gel precipitation on the formation of the pore structure of the xerogel [12]. The processes of the formation of the texture do not stop after gel precipitation. They also occur at the stage of its aging (ripening) in the intermicellar medium.

The goal of this work was to study the regularities of the formation of zirconium dioxide pore structure at the stage of aging of the gel prepared by precipitation, as well as during the subsequent thermal treatment of the xerogel.

## EXPERIMENTAL

The samples of zirconium dioxide were prepared by precipitation from an aqueous solution of zirconyl chloride ( $\approx 110$  g  $\text{ZrO}_2$ /l), the most often used zirconium compound, by a 12.5% aqueous solution of ammonia, along with vigorous stirring. The solutions of zirconium chloride were heated before precipitation.

$\text{ZrO}_2$  gels used for further aging were prepared at pH 8 and 4 and a temperature of 80°C. The precipitates were washed with distilled water until the disappearance of chloride ions from the washing water ( $\sim 10$  H<sub>2</sub>O/100 g  $\text{ZrO}_2$ ). An aqueous suspension with a concentration of 50 g  $\text{ZrO}_2$ /l was prepared and kept at 80°C and neutral pH. The suspension was aged and vigorously stirred. The suspension was sampled at known intervals, and the precipitate was filtered off. Granules were formed by extrusion through a 4-mm nozzle and dried to air-dry state and at 150°C in an oven for 12 h. Several samples were calcined in a muffle at 500°C for 4 h.

The pore structure of xerogels was studied by low-temperature nitrogen adsorption on an automatic DigiSorb-2600 Micromeritics instrument. The true density  $\rho$  (g/cm<sup>3</sup>) was measured against helium on an Auto-Pycnometer-1320 Micromeritics instrument. The total pore volume  $V_\Sigma$  (cm<sup>3</sup>/g) and porosity  $\varepsilon$  (cm<sup>3</sup>/cm<sup>3</sup>) were calculated from the values of bulk density  $\Delta$  (g/cm<sup>3</sup>) and true density ( $V_\Sigma = 0.6/\Delta - 1/\rho$ ). The surface areas of mesopores  $S_\alpha$  and macropores  $S_\alpha$  (m<sup>2</sup>/g) and the micropore volume  $V_\mu$  (cm<sup>3</sup>/g) were calculated from the adsorption isotherms by the comparative method. The predominant pore size ( $d$ , nm) was calculated from the desorption branch of the isotherm according to the classical Barett–Joyner–Halenda (BJH) method [13]. The limiting volume of the sorption space  $V_s$  (cm<sup>3</sup>/g) corresponds to the fraction of the  $V_\Sigma$  volume with pore diameters less than 100 nm.

**Table 1.** The effect of the time of gel aging and pH of precipitation on the textural parameters of the  $\text{ZrO}_2$  xerogel

No.	$t, \text{h}$	pH	$\rho, \text{g/cm}^3$	$S_\alpha, \text{m}^2/\text{g}$	$V_\mu, \text{cm}^3/\text{g}$	$V_s, \text{cm}^3/\text{g}$	$V_{\text{me}}, \text{cm}^3/\text{g}$	$\epsilon$	$\beta$
1	0	8	4.45	184.4	0.018	0.130	0.082	0.36	15.6
2	3	8	4.34	271.8	0.009	0.184	0.142	0.44	14.8
3	8	8	4.32	309.1	0	0.205	0.173	0.47	11.4
4	25	8	4.33	350.3	0	0.268	0.270	0.54	10.3
5	0	4	3.92	53.9	0.029	0.071	0.033	0.22	27
6	3	4	3.96	85.5	0.034	0.086	0.035	0.25	—
7	5	4	3.95	86.6	0.037	0.089	0.033	0.26	24
8	10	4	3.97	91.6	0.040	0.094	0.033	0.27	22
9	22	4	4.00	93.2	0.036	0.099	0.044	0.28	—

The X-ray phase analysis was carried out on a URD-63 diffractometer with filtered  $\text{CuK}_\alpha$  radiation, and the electron-microscopic study was performed on a JEM-2010 instrument.

The experimental findings for the xerogels obtained from aged gels are presented in Table 1.

## RESULTS AND DISCUSSION

As can be seen from Table 1, for the sample precipitated at pH 8, the xerogel texture changes significantly with an increase in the time of hydrogel aging  $t$ : the surface area of mesopores increases and the micropore volume decreases simultaneously; then, micropores disappear.

The limiting volume of sorption space  $V_s$  also increases. The shape of the nitrogen adsorption iso-

therm (Fig. 1) indicates that this value corresponds to the total pore volume in the sample. The porosity ( $\epsilon$ ) of the xerogels also increases. If the pore volume calculated from the desorption branch of the adsorption isotherm according to the BJH method is assumed to be the mesopore volume  $V_{\text{me}}$  only (Table 1), then it is obvious that the total pore volume increases due to an increase in the volume of mesopores. Note that the supermicropore volume calculated as  $V_{\text{sp}} = (V_s - V_{\text{me}} - V_\mu)$  does not change during aging for 8 h and equals  $\sim 0.03 \text{ cm}^3/\text{g}$ . Further gel aging (for 25 h) results in the disappearance of supermicropores.

Table 1 also shows the extent of shrinking of the volume between particles in a hydrogel in the course of drying ( $\beta$ ). This characteristic was calculated as follows:

$$\beta = \epsilon_h / \epsilon_x (l_h / l_x)^3,$$

where  $\epsilon_x$  is the porosity of the xerogel formed,  $\epsilon_h$  is the calculated volume of the liquid phase per the unit hydrogel volume,  $l_h$  and  $l_x$  are the linear sizes of the hydrogel and xerogel granules. It is seen that the extent of shrinking decreases with an increase in the time of aging, pointing to the growth in the extent of the gel aggregation or a change in the morphology of particles during aging.

As shown in [14], the porosity of the random packing of the particles increases significantly with an increase in anisotropy. For example, the porosity of packing of the cylinder particles increases when the ratio between their length and diameter increases. Hence, one can expect that an enhancement of the anisotropy of the oxide particles during aging would also lead to the growth of the xerogel porosity and simultaneously to a decrease in the extent  $\beta$  of shrinking of the volume between particles.

Figure 2 shows the curves of the differential pore size distribution of the mesopore volume for the samples. It follows from Fig. 2 that the zirconium dioxide xerogels form a narrow-pore structure. With an increase in the time of aging, an increase in the mesopore volume is accompanied by the reconstruction of the pore struc-

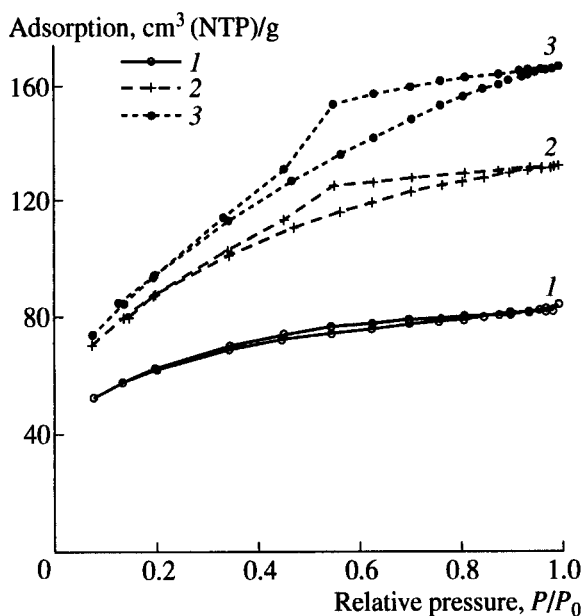


**Fig. 1.** Nitrogen adsorption isotherms on the zirconium dioxide xerogels precipitated by an ammonia solution at pH 8; time of aging (h): (1) 0, (2) 8, and (3) 25.

ture. While mesopores with a diameter of  $\sim 2$  nm prevailed in the initial xerogel, the pores with a diameter of 4 nm appear during aging.

Thus, the aging of a zirconium hydroxide hydrogel results in a successive decrease in the volume of the most narrow pores: primarily micropores and then supermicropores. An increase in the surface area, together with only a slight change in the true density, indicates the disintegration (dispersion) of initially large particles of the oxide whose average size was  $\sim 7$  nm according to the adsorption data. In the course of aging for 25 h, the average size of primary particles decreases to  $\sim 4$  nm; that is, about five particles are formed from one precipitated particle of  $\text{ZrO}_2$ .

The dispersion of initially amorphous primary particles may occur as a result of the reconstruction of the crystalline phase of zirconium dioxide present in the sample. The data on the true density shows that, in the course of aging, the weight fraction of the crystalline phase does not change significantly during the time of observation. According to X-ray diffraction data, one can only presume the genesis of highly dispersed and apparently defect crystalline particles. An ambiguity in the findings is due to a typical broad halo in diffraction patterns.

On the basis of the electron microscopic data, one can conclude that the precipitated sample does not contain the crystalline phase, but defect crystalline particles with diameters of 7–9 nm and that the disordered internal structure are formed in the course of aging.

Micrographs show that the shape of these particles is far from being spherical and that they are in fact close to flat elongated disks. The anisotropy of this particle is higher than that of a spherical particle. Hence, possible mutual orientation and intimate mating that usually results in more dense packing are negligible due to the small volume fraction of the crystalline phase in the xerogel that does not exceed 30 wt %. One can conclude that a change in the morphology of the crystal particles is the reason for the enhanced porosity of the zirconium dioxide xerogels during aging.

Note that the formation of the flat plate-like (sometimes called two-dimensional) particles of zirconium dioxide was reported in [15, 16]. The formation of such particles is usually observed during hydrothermal treatment and is accompanied by an increase in the surface area. Consequently, the plate shape of the zirconium dioxide crystal particles is a rather abundant morphology of the monoclinic modification of zirconium dioxide.

Aging of a zirconium dioxide gel precipitated at pH 4 is accompanied by other fundamental changes in the xerogel texture and true density. As can be seen from Table 1, the  $\rho$  value increases monotonically but remains lower than that in the case of pH 8. This is likely due to the greater fraction of the amorphous constituent of the xerogel skeleton retained and its slight changes during aging. The presence of a small amount

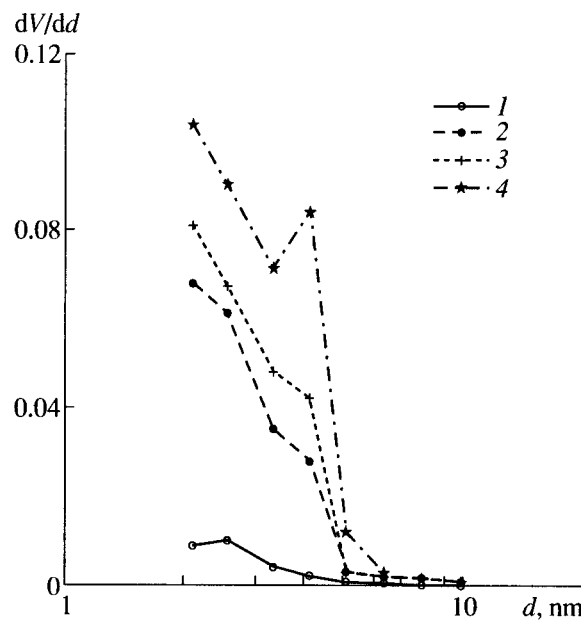


Fig. 2. Differential pore size distribution for the samples of zirconium dioxide obtained from hydrogels precipitated by an ammonia solution at pH 8 and aged during (1) 0, (2) 3, (3) 8, and (4) 25 h.

of low-molecular species as the oxide precursors also should not be ruled out; this seems to be possible for this range of pH values.

Figure 3 presents the nitrogen adsorption isotherms for the series of samples precipitated at pH 4. The typical irreversibility of adsorption isotherms in the whole range of relative adsorbate pressures, which is associated with the activated diffusion of the nitrogen molecules in the micropore space of xerogels, is retained during aging. Notably, the textural parameters of the xerogels listed in Table 1 were calculated from the desorption branch of the isotherm, which was probably more equilibrated in this case.

Along with an increase in the  $S_\alpha$  value, the micro- and supermicropores volumes also increase, while the small mesopore volume  $V_{me} \approx 0.03 \text{ cm}^3/\text{g}$  virtually remains constant. Correspondingly, the total porosity of the xerogel also increases during aging. The mesopore volume slightly increases only due to prolonged aging (22 h).

It is interesting that, in the initially mesoporous xerogels synthesized at pH 8, it is the mesopore fraction of the pore space that significantly increases during aging due to an increase in the volume and size of these pores. In the initially microporous xerogels obtained at pH 4, mostly the micropore volume increases, while the mesopore fraction of the pore space slightly changes.

The formation of the oxide skeleton continues during aging of the hydrous gel at 80°C. The polymorphic transformations in the bulk of primary particles (in particular, a change in their morphology), accompanied by the dispersion of particles, occur in the  $\text{ZrO}_2$  precipitate

**Table 2.** The textural parameters of the  $\text{ZrO}_2$  samples aged at the gel stage and calcined at 500°C

Sample*	$\rho$ , g/cm <sup>3</sup>	$S_\alpha$ , m <sup>2</sup> /g	$V_s$ , cm <sup>3</sup> /g	$d$ , nm	$\epsilon$ , cm <sup>3</sup> /cm <sup>3</sup>	$\Delta V$ , cm <sup>3</sup> /g	$\beta$
5	5.61	32.6	0.088	5.7	0.33	0.076	0.98
6	5.64	39.4	0.091	7.1	0.34	0.075	0.97
7	5.66	46.4	0.095	7.3	0.35	0.076	0.94
8	5.68	48.0	0.094	7.4	0.35	0.076	0.99

\* The number of the sample corresponds to that in Table 1.

formed at pH 8. The phase formation processes continue to occur in the precipitate obtained at pH 4, which contained a significant amount of low-molecular fragments as oxide phase precursors.

As one would expect, the density increased upon thermal treatment at 500°C of the xerogels aged at the gel stage (Table 2). The main textural parameters also changed. A comparison of the experimental data for the xerogels before and after thermal treatment gives evidence for the complete disappearance of micropores and a significant decrease in the specific surface area. The limiting volume of the sorption space  $V_s$  usually does not change markedly (Fig. 4). It is more correct to compare the textural parameters for genetically related samples, whose true densities changed considerably during the genesis, by using the porosity values (when comparing the pore volumes) or the average calculated values for the particle sizes with approximating particles by spheres (when comparing the surface areas), rather than by attributing these parameters to the weight unit.

It follows from Tables 1 and 2 that the porosity of the xerogels increases during thermal treatment because the additional pore volume arises due to a change in the true density of the xerogel skeleton. This volume can be estimated using the expression  $\Delta V = (1/\rho_i - 1/\rho_f)$ , where  $\rho_i$  and  $\rho_f$  are the initial and final densities of a material, respectively (Table 2). Note that this value of  $\Delta V$  is the limiting value which is achieved only in the case of the ideal pseudomorphic transformation without changing the chemical composition of the sample. The preservation of the external sizes of a granule is the necessary condition for the ideal pseudomorphism.

In the case considered, the real porosity of calcined xerogel is lower than that expected from the calculation of the overall porosity of the aggregated structure according to the equation

$$\epsilon = \epsilon_p + \epsilon_i(1 - \epsilon_p) = \epsilon_i + \epsilon_p(1 - \epsilon_i),$$

proceeding from the values of the initial ( $\epsilon_i$ ) and newly formed porosity ( $\epsilon_p$ ). Hence, the main conditions for

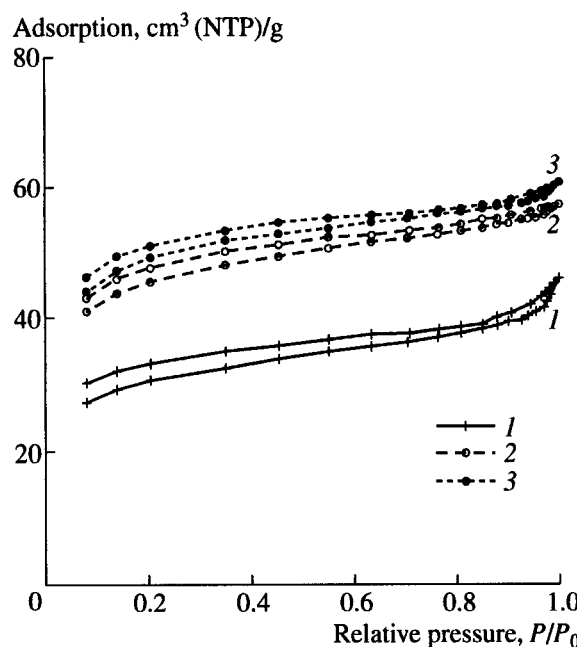


**Fig. 3.** Nitrogen adsorption isotherms on the zirconium dioxide xerogels precipitated by an ammonia solution at pH 4; time of aging (h): (1) 0, (2) 5, and (3) 10.

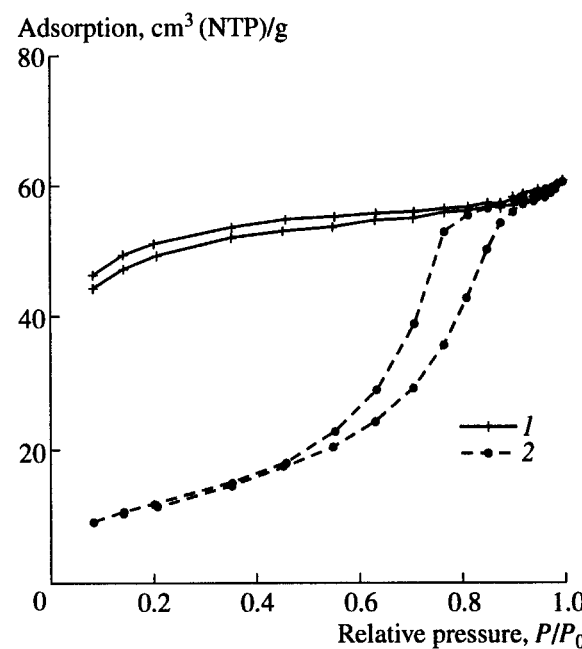


**Fig. 4.** Nitrogen adsorption isotherms on the zirconium dioxide xerogel (1) aged during 10 h at the gel stage and (2) after calcination of the sample at 500°C.

the ideal pseudomorphism are not achieved in this case. Indeed, the sizes of calcined granules indicate that they significantly decrease during calcination. The calculated shrinking of the pore space  $\beta$  is close to unity (Table 2). This is probably associated with the compensation for the formation of new pores by the simultaneous shrinkage of the skeleton during thermal sintering.

To summarize, we conclude that the calcination of zirconium dioxide prepared by the procedure considered in this paper is accompanied by the diffusional process of bulk sintering at as low temperature as 500°C, with all typical features finally resulting in the considerable reconstruction of the pore space in the xerogel.

#### ACKNOWLEDGMENTS

We are grateful to S.V. Tsybulya and G.N. Kryukova for their help in experiments.

#### REFERENCES

1. Turlier, P., Dalmon, J.A., Martin, G.A., and Vergnon, P., *Appl. Catal.*, 1987, vol. 29, no. 2, p. 305.
2. Mercera, P.D.L., Van Ommen, J.G., Doesburg, E.B.M., *et al.*, *Appl. Catal.*, 1991, vol. 78, no. 1, p. 79.
3. Ivanova, A.S., Bobrova, I.I., Moroz, E.M., *et al.*, *Kinet. Katal.*, 1997, vol. 38, no. 1, p. 114.
4. Tanabe, K. and Yamaguchi, T., *Catal. Today*, 1994, vol. 20, no. 2, p. 185.
5. Rutman, D.S., Toropov, Yu.S., Plesher, S.Yu., and Polezhaev, Yu.M., *Vysokoognepornye materialy iz dioksida tsirkoniya* (Hearthstone from Zirconium Dioxide), Moscow: Metallurgiya, 1985.
6. Metcalfe, I.S., *Catal. Today*, 1994, vol. 20, no. 2, p. 283.
7. Ivanova, A.S., Moroz, E.M., and Litvak, G.S., *Kinet. Katal.*, 1992, vol. 33, nos. 5–6, p. 1208.
8. Yamaguchi, T., *Catal. Today*, 1994, vol. 20, no. 2, p. 199.
9. Pechenyuk, S.I. and Kalinkina, E.V., *Izv. Akad. Nauk, Ser. Khim.*, 1996, no. 11, p. 2653.
10. Krylov, O.V., *Ross. Khim. Zh.*, 1997, vol. 41, no. 3, p. 124.
11. Stiles, A.B., *Catalyst Supports and Supported Catalysts: Theoretical and Applied Concepts*, Boston: Butterworths, 1987.
12. Gavrilov, V.Yu. and Zenkovets, G.A., *Kinet. Katal.*, 1996, vol. 37, no. 4, p. 617.
13. Barrett, E.P., Joyner, L.B., and Halenda, E., *J. Am. Chem. Soc.*, 1951, vol. 73, no. 1, p. 373.
14. Fenelonov, V.B. and Zagrafskaya, R.V., *Modelirovaniye poristykh materialov* (Modeling of Porous Materials), Kurnaukhov, A.P., Ed., Novosibirsk: Inst. of Catal., 1976, p. 60.
15. Clearfield, A., *Rev. Pure Appl. Chem.*, 1964, vol. 14, no. 1, p. 91.
16. Livage, J., Doi, K., and Mazieres, C., *J. Am. Ceram. Soc.*, 1968, vol. 51, no. 6, p. 349.